B7-H1 Promotes the Functional Effect of Human Gingiva-Derived Mesenchymal Stem Cells on Collagen-Induced Arthritis Murine Model

Wenbin Wu,[1,6] Ze Xiu Xiao,[1,6] Donglan Zeng,[1] Feng Huang,[1] Julie Wang,[2] Yanying Liu,[3] Joseph A. Bellanti,[4] Nancy Olsen,[5] and Song Guo Zheng[2]

[1]Department of Clinical Immunology, The Third Affiliated Hospital of Sun Yat-sen University, Guangzhou 510630, China; [2]Department of Internal Medicine, Ohio State University College of Medicine and Wexner Medical Center, Columbus, OH 43210, USA; [3]Department of Rheumatology & Immunology, Peking University People's Hospital, Beijing 100044, China; [4]Departments of Pediatrics and Microbiology-Immunology and the International Center for Interdisciplinary Studies of Immunology (ICISI), Georgetown University Medical Center, Washington, DC 20057, USA; [5]Department of Medicine, Penn State University Hershey Medical Center, Hershey, PA 17033, USA

Recent studies found that mesenchymal stem cells (MSCs), by virtue of their tissue recovery and immunoregulatory properties, have shown a broad prospect for applications in various autoimmune and degenerative diseases. Although the potential therapeutic use of MSCs is considerable, studies and clinical treatment efficacy are preliminary due to the heterogeneity of MSCs. Herein, based on RNA-sequencing (RNA-seq) and single cell sequence properties, we demonstrated that B7-H1 plays an important role in the immunosuppressive function of human gingiva-derived mesenchymal stem cells (GMSCs) in a collagen-induced arthritis murine model that is dependent on STAT3 signaling. Our data offer convincing evidence that B7-H1 expression by GMSCs helps to identify a new subpopulation of MSCs with a greater immunosuppressive property. The approach provides a unique and additional strategy for stem cells-based therapies of autoimmune and other inflammatory diseases.

INTRODUCTION

Rheumatoid arthritis (RA), a chronic inflammatory autoimmune condition characterized by polyarticular arthritis and bone damage primarily affecting the small diarthrodial joints, is a leading worldwide cause of disability.[1,2] The primary therapeutic agents currently used to treat RA are the disease-modifying antirheumatic drugs (DMARDs), which mainly target reducing the progression of structural damage and the biologic therapies that neutralize the inflammatory-inducing effects of cytokines, e.g., the tumor necrosis factor alpha (TNF-α) inhibitors. Although these agents have been proven to dramatically improve the outcome of RA, unfortunately, they are not curative for the disorder.[3–5] Novel and more effective therapies are clearly needed.

Mesenchymal stem cells (MSCs) are stromal cell progenitors, which display significant regenerative, immunomodulatory, and tissue-protective properties and are being extensively investigated in patients suffering from autoimmune and other inflammatory disorders.[6–9]

The most common source of MSCs are bone marrow, adipose, and umbilical tissues, and their immunosuppressive functions are based upon their ability to inhibit the proliferation and activation of T cells, dendritic cells, natural killer cells, macrophages, and inflammatory cells, as well as their capacity to promote the induction of regulatory T cells.[10–15] Gingiva-derived mesenchymal stem cells (GMSCs) are a recently identified subset of MSCs. In contrast to other MSC subpopulations, they are more easily accessible and display more rapid *in vitro* proliferative properties.[16] More importantly, GMSCs have demonstrated superior immunoregulatory function relative to bone-marrow-derived mesenchymal stem cells (BMSCs).[17] We and others have recently documented that GMSCs are able to treat several diseases in mouse and humanized animal models through decreasing inflammatory T cells, dendritic cells, macrophages, osteoclasts, and increasing regulatory T cells.[18–24,25] Although the potential therapeutic application of these MSCs is considerable, their clinical feasibility is limited both by the heterogeneity of MSCs, as well as side effects, which have been observed in some clinical trials.[26,27] Functional heterogeneity of MSCs has been observed in different individuals,[28] and subsets characterized by different biomolecular markers have also been discovered.[29] The use of specific subsets of MSCs can eliminate certain interfering factors, thereby exerting their special functions and designing more effective therapies. Therefore, it is important to further subdivide MSCs and characterize their functional differences in order to develop strategies for treating various diseases using standardized MSCs.

B7-H1 (PD-L1) is a costimulatory molecule widely expressed on activated T cells, B cells, monocytes, and many types of cancer cells[30,31]
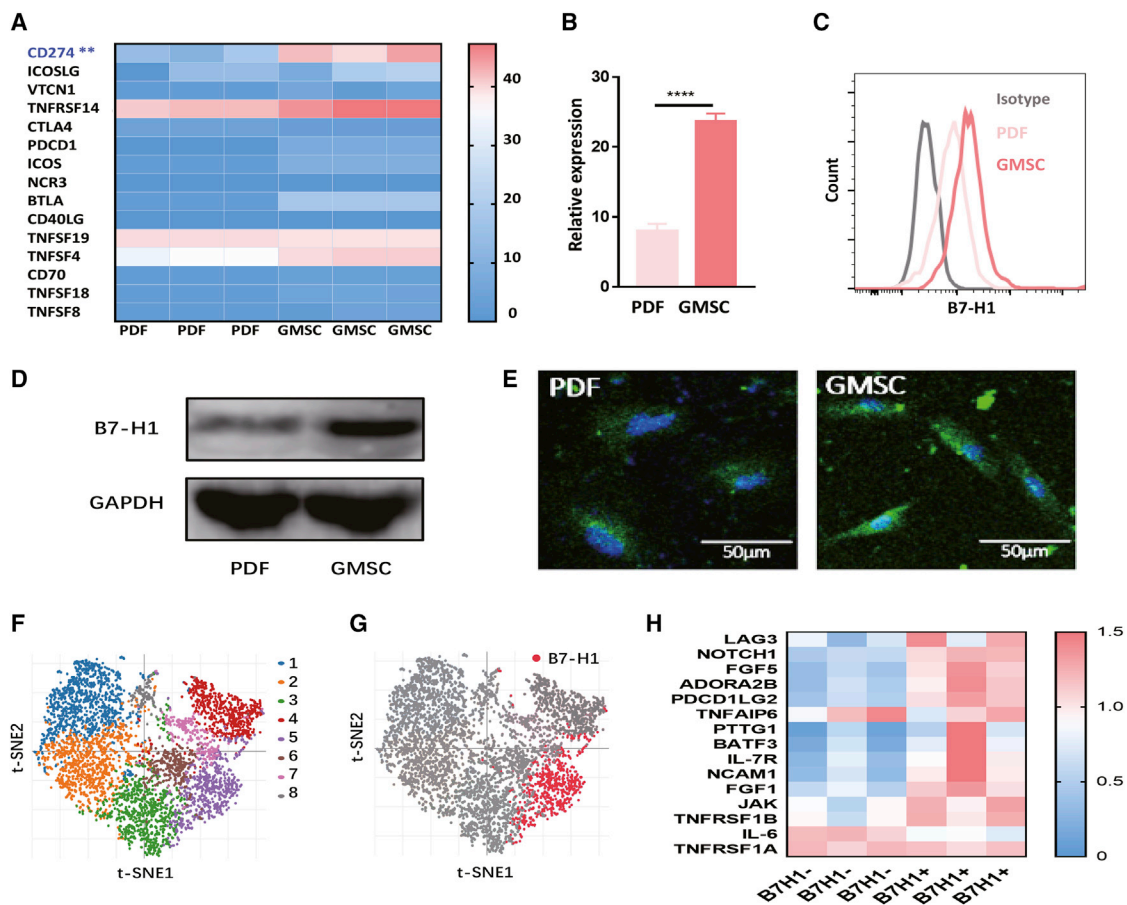
Figure 1. B7-H1 Expression Is the Marker of a Subpopulation of GMSCs

GMSCs (gingiva-derived mesenchymal stem cells) and PDFs (prepuce derived fibroblasts) derived from three different individuals. Fresh cells or resuscitated stored cells from the third to the fifth passages were used in the experiments. (A) RNA sequence heatmap for GMSCs and control cells PDFs. (B) B7-H1 expression on GMSCs and PDFs was determined by quantitative RT-PCR. (C) B7-H1 expression on GMSCs and PDFs was determined by flow cytometry. (D) B7-H1 expression on GMSCs and PDFs was determined by western blotting. (E) B7-H1 expression on GMSCs and PDFs was detected by immunofluorescence. (F) Eight GMSC clusters, t-distributed stochastic neighbor embedding (t-SNE) of GMSCs, colored by clustering. (G) B7-H1 expression in single cell sequence clusters. (H) Single cell sequence heatmap for GMSC clusters. The results represent three independent experiments (mean ± SEM), *p < 0.05, **p < 0.005, ***p < 0.0005, ****p < 0.0001 by t test or ANOVA test.

that displays a strong negative effect on immune actions[32,33] after binding with its cognate PD-1 molecule, which is expressed mainly on T cells.[34] Previous studies have revealed that MSCs exert a protective allograft transplant response mediated by suppression of inflammatory T cells probably through the B7-H1/PD-1 pathways.[35–38] It would be of interest to examine whether the purified B7-H1[+] MSC subpopulation holds greater immunosuppressive properties to provide a unique and additional strategy for stem cells-based therapies.

Herein, we demonstrated that GMSCs could be sorted into B7-H1[high] and B7-H1[low] subpopulations and that the immunomodulatory function of GMSC is highly related to B7-H1 signaling. In a collagen II-induced arthritis (CIA) murine model, we observed that blockage of B7-H1 signaling by specific antibody was associated with marked abrogation of GMSC immunosuppression. Conversely, the immunosuppressive effect was enhanced when B7-H1 was overexpressed. We

further found that the B7-H1 signaling-strengthening effect on the immune regulation of GMSC was dependent upon the STAT3 pathway. These results suggest that B7-H1 signaling plays an important role in the immunosuppression of GMSC. Thus, B7-H1 may not only be an excellent marker to identify the subpopulation of GMSCs that exhibit immunomodulatory effects but also B7-H1[high] GMSC might provide a more effective cell that could be considered for the treatment of patients with rheumatoid arthritis and other immune-mediated diseases.

RESULTS

B7-H1 Expression Is the Marker of a Subpopulation of GMSCs

We used several techniques to test the B7-H1 expression level in GMSCs. RNA-seq showed that the transcriptional level of B7-H1 was significantly higher in GMSCs than in control cells, prepuce-derived fibroblasts (PDFs; Figure 1A). We validated the expression

level difference by quantitative RT-PCR (Figure 1B). Using flow cytometry, western blotting, and immunofluorescence technology, we further observed that the B7-H1 protein level of GMSCs is also higher relative to control (Figures 1C–1E). Thus, we provide evidence that GMSCs express greater levels of B7-H1 with potential functional consequences.

Due to the heterogeneity of GMSCs, we further used a single cell sequence to verify GMSC subpopulations. There were eight GMSC clusters identified using t-distributed stochastic neighbor embedding (Figure 1F). We found that the expression of B7-H1 in cluster 5 was significantly higher than that in other clusters (Figure 1G). Interestingly, based on single cell sequence properties, we also noted that the expression of multiple immune related molecules was different in B7-H1^{high} and B7-H1^{low} subsets (Figure 1H). Thus, the B7-H1 expression may be an ideal surface molecule marker to reflect the immunosuppressive function of GMSC subpopulations.

B7-H1^{high} Expressed GMSC Showed Higher Suppressive Ability Than B7-H1^{low} Expressed GMSC in CIA Mice

Given that B7-H1 is a crucial negative co-stimulatory molecule involved in the immunoregulation of T cell responses,[34] we next sought to determine whether B7-H1 expression in GMSC is functionally relevant. GMSC were sorted into B7-H1^{high} and B7-H1^{low} populations based on their fluorescence intensity (Figures S1A–S1C). Using a previously described allogeneic mixed lymphocyte cell culture system,[39,40] we noted that B7-H1^{high} GMSC had a more efficient suppressive function against T cells proliferation compared with the B7-H1^{low} population (Figure 2A). The B7-H1^{high} population also had greater suppressive effect on interferon-γ (IFN-γ) production by T cells compared to B7-H1^{low} subset (Figure 2B). These results demonstrate that the B7-H1^{high} GMSC display more potent suppressive ability than B7-H1^{low} counterpart *in vitro*.

We next compared the suppressive effect of the two subsets of GMSCs on collagen-induced arthritis (CIA) disease progression (Figure S1D). We found no significant difference between the B7-H1^{low} GMSC treatment group and the model group in severity scores, antibody level, cytokines, and histology. However, we observed that B7-H1^{high} GMSCs had a significant therapeutic effect compared to B7-H1^{low} GMSC (Figure 2C). The levels of the auto-immune antibody (anti-dsDNA antibody) and the specific antibody (anti-CII antibody) showed higher reduction in the B7-H1^{high} GMSC treatment group compared with the B7-H1^{low} GMSC in CIA mice (Figure 2D), and the inflammatory cytokines, including interleukin-17a (IL-17a), TNF, IFN-γ, and IL-6, showed greater decrease in B7-H1^{high} GMSC treatment group mice sera, while the anti-inflammatory cytokine IL-10 showed the opposite changes (Figure 2E). The gross appearance of the CIA mice hind limbs was consistent with significant remission in B7-H1^{high} GMSC treatment group compared to lesser effect in the B7-H1^{low} GMSC group (Figure 2F). Micro computed tomography (CT) imaging to determine pathologic changes in the feet of the CIA mice showed that the B7-H1^{high} GMSC-infused CIA mice showed slight narrowed joint spacing in

the feet and mild bone erosion compared with the B7-H1^{low} GMSC treatment group (Figure 2F). Histological and quantitative analysis of the ankle joints of the CIA mice showed a significant amelioration in synovitis, pannus formation, and destruction of the bones and cartilage on the B7-H1^{high} GMSC therapeutic group mice compared to the other two groups (Figure 2F). We performed toluidine blue staining and tartrate-resistant acid phosphatase (TRAP) staining to measure the extent of the cartilage damage in joints and the osteoclasts, the joint destruction exhibited higher alleviation in B7-H1^{high} GMSC therapeutic group mice (Figure 2F). The weight of spleens and lymph nodes from the B7-H1^{high} GMSC treatment group mice showed significant decrease compared with the CIA model and B7-H1^{low} GMSC group mice (Figure S1E).

Consistent with the auto-antibodies and specific anti-CII antibodies levels, the B cells (B220$^+$) and plasma cells (CD38$^+$CD138$^+$) decreased in B7-H1^{high} GMSC treatment group CIA mice spleen or lymph node than the other two groups (Figure S1F). The inflammatory T helper cells (CD4$^+$IFN-γ^+ and CD4$^+$IL-17a$^+$) were decreased in the spleens or lymph nodes from B7-H1^{high} GMSC group CIA mice, while the anti-inflammatory regulatory T cells (Tregs, CD4$^+$Foxp3$^+$) or nTregs (CD4$^+$Fxop3$^+$Helios$^+$) showed a significant increase in the B7-H1^{high} expressed GMSC treatment group (Figure S1F). Taken together, our results suggest that B7-H1 exerted a critical role in the immune suppression of the GMSCs *in vitro* and *in vivo*.

Antagonist of B7-H1 Impaired the Suppressive Effect of GMSC on CIA Mice

To further study the role of B7-H1 in GMSC, we used the B7-H1-specific antagonist antibody to block B7-H1 signaling (Figure S2A). We observed that the suppressive effect of GMSC on T cell proliferation was mostly abolished when the B7-H1 signaling pathway in GMSCs was blocked (Figure 3A). Furthermore, the decreased cytokine secretion including IL-17a, IFN-γ, and TNF from T cells was significantly recovered when the B7-H1 antagonist antibody was used to pretreat the GMSCs (Figure 3B).

We next investigated the immunosuppression of GMSCs after the B7-H1 signaling was blocked in CIA mice. The B7-H1-specific antagonist antibody pretreated GMSCs and control unpretreated GMSCs were transferred to the CIA mice on day 14 after the CII immunization, respectively. We found that the suppressive effect of GMSCs on CIA mice was significantly impaired as the B7-H1 signaling in GMSCs was previously blocked (Figure 3C). The reduction of autoantibodies (anti-dsDNA antibody and the specific anti-CII antibody) in the GMSCs treatment group was also significantly abolished (Figure 3D), and the inflammation cytokines such as IL-17a, TNF, IFN-γ, and IL-6 showed higher level in CIA when the B7-H1 pathway was blocked on the GMSCs. Interestingly, levels of the anti-inflammation cytokine IL-10 showed diametric decrease in the CIA mice with GMSC-B7-H1 blocked treatment (Figure 3E).

As shown in Figure 3F, the GMSCs alleviated the destructive phases of the polyarthritis in the hind limbs and ameliorated the decreases of
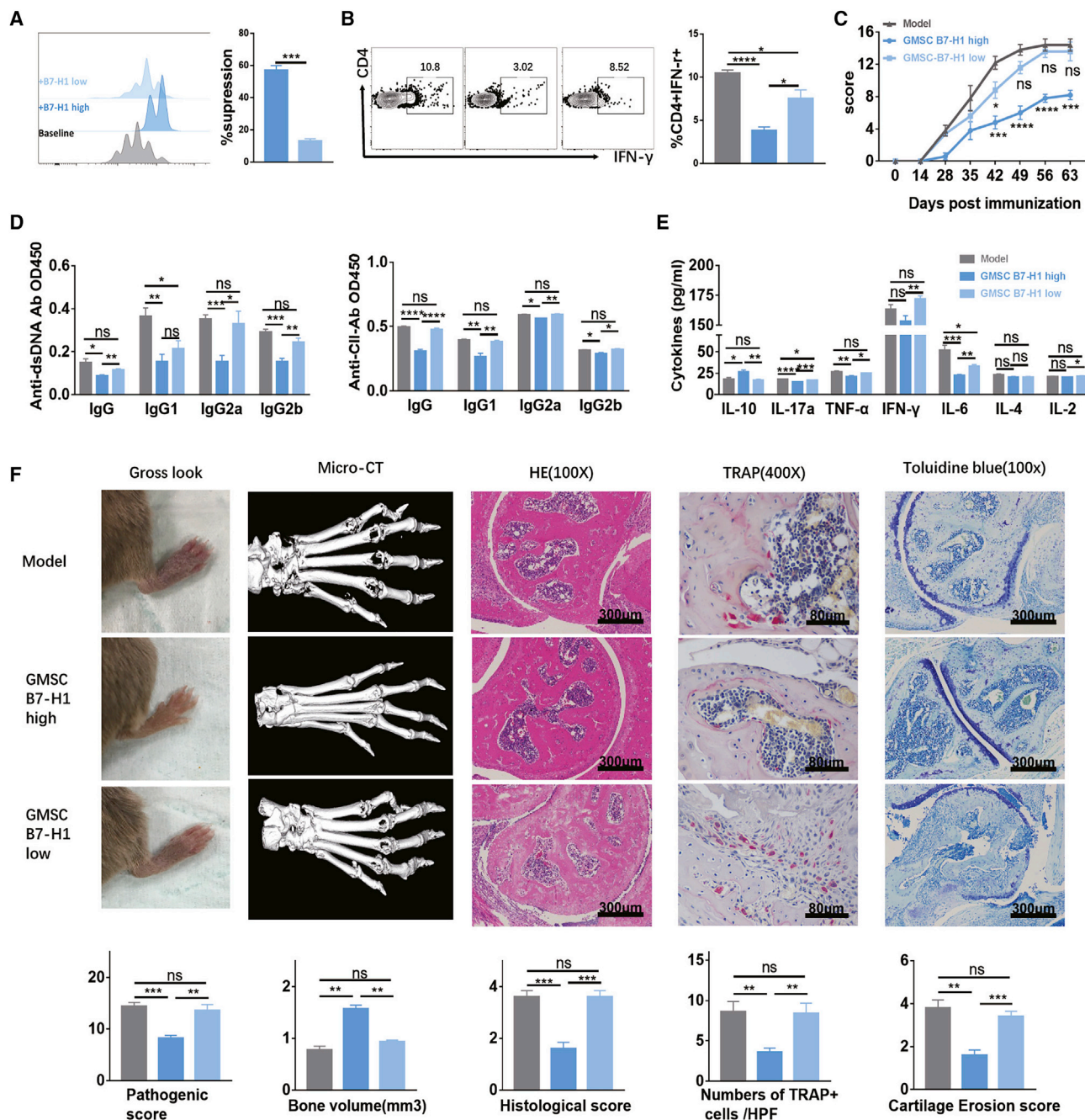
Figure 2. B7-H1^high GMSC Showed High Suppressive Ability than B7-H1^low GMSC

(A and B) GMSCs were sorted into B7-H1^high and B7-H1^low two populations by flow cytometry. Mouse splenic T cells and antigen-presenting cells (APCs) were isolated with nylon wool. T cells labeled with CFSE were stimulated with anti-CD3 mAb (Biolegend, 1 μg/mL) and mitomycin (Sigma, M4287) pretreated APCs. GMSCs were co-cultured with T cells-APCs on the ratio 1:10 for 72 h. (A) The suppression on T cells proliferation in different groups was determined by flow cytometry. (B) IFN-γ secretion from T cells in different groups was determined by flow cytometry. (C–F) CIA was induced in DBA/1 mice, after 14 days of immunization, mice were treated with B7-H1^high or B7-H1^low GMSCs or PBS (model) and euthanized on day 63, and the mice in the same group received the same cells from the same donor. (n = 5 in one individual experiment). (C) The clinical scores of CIA mice changed with time. (D) The anti-dsDNA antibody and anti-CII antibody levels of the CIA mice were detected using ELISA. (E) The cytokines levels of the serum from the CIA mice were quantified by CBA kit. (F) Representative gross look, micro CT, H&E staining, TRAP, and toluidine blue stained joint tissue sections from the CIA mice. And the scores of synovial inflammations, cartilage damage, bone erosion, and the total number of TRAP-positive cells in the field were counted in each group. The results represent three independent experiments (mean ± SEM), *p < 0.05, **p < 0.005, ***p < 0.0005, ****p < 0.0001 by t test or ANOVA test.
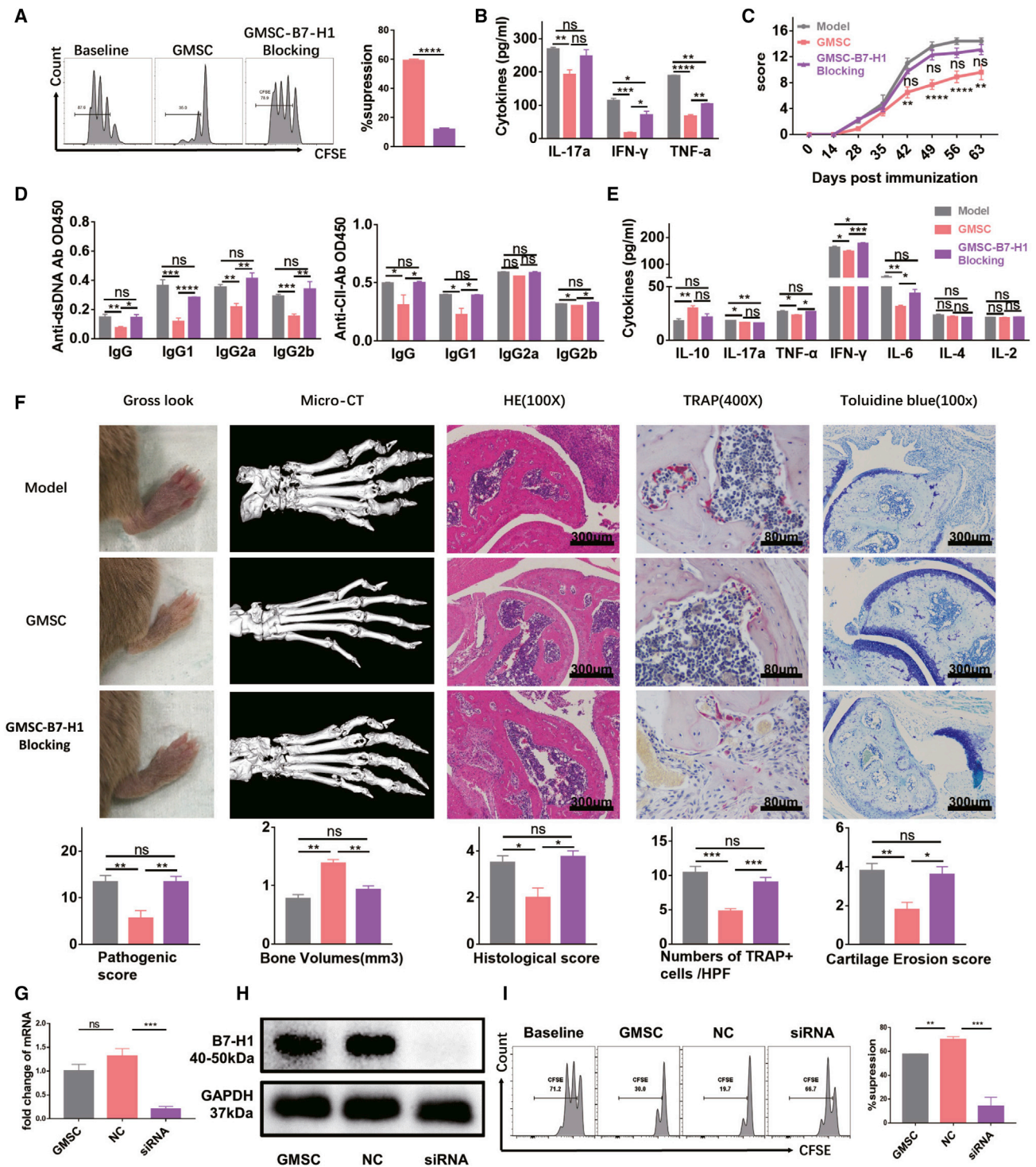
Figure 3. Antagonist of B7-H1 on GMSC Abolished the Suppression Ability of GMSCs on CD4+ T Cells

(A and B) GMSC were pretreated with B7-H1 blocking antibody (Biolegend, 10 μg/mL) overnight, then co-cultured with T cells-APCs on the ratio 1:10 for 72 h. (A) The suppression on T cells proliferation in different groups was determined by flow cytometry. (B) The cytokines (IL-17a, TNF-α, and IFN-γ) secretion from T cells in different groups was determined by flow cytometry. (C–F) CIA was induced in DBA/1 mice, after 14 days of immunization, mice were treated with GMSC, B7-H1 blocking GMSC or PBS (model), and euthanized on day 63, and the mice in the same group received the same cells from the same donor (n = 5 in one individual experiment). (C) The clinical

(legend continued on next page)

the spacing between the metatarsals and phalanges compared with model CIA mice, which is consistent with our previous findings.[4] Nevertheless, B7-H1 antagonist antibody pretreated GMSCs did not show the suppressive effect on the CIA mice. Accordingly, we observed that the splenomegaly and lymphadenopathy were abated in the GMSC-treated CIA mice, B7-H1 signaling that blocked GMSCs showed almost the same pathogenic changes as for model CIA mice (Figure S2B). The plasma cells and B cells were decreased in the GMSC treatment CIA mice, and the other inflammatory cells such as CD4$^+$IFN-γ^+ T cells and CD4$^+$IL-17$^+$ T cells were decreased in the GMSC treatment CIA mice as well (Figure S2C). Additionally, the Tregs (including nTregs) were increased in the GMSC treatment CIA mice. On the contrary, the B7-H1 signaling blocked GMSC group mice and showed parallel pathogenic changes with model CIA mice (Figure S2C). These results show that blocked B7-H1 signaling on the GMSC impaired or even abolished the suppressive function of GMSCs.

To make the results more definitive, we used small interfering RNA (siRNA) to knock down B7-H1 in GMSCs to confirm the function in vitro experiments (Figures 3G–3I). We additionally evaluated the inflammatory bowel disease model to further show that GMSC treatment did alleviate inflammatory colitis, at least partly, via B7-H1 (Figure S3).

Overexpressed B7-H1 Increased the Immunosuppression of GMSCs

Previous studies had demonstrated that IFN-γ could significantly induce the B7-H1 expression.[41] Here we used a similar protocol to show that IFN-γ indeed also induced the B7-H1 expression on GMSCs (Figures S4A–S4D). We next explored the function of the B7-H1 overexpression in GMSCs, using a T cell proliferation experiment. We observed that IFN-γ-pretreated GMSCs exerted stronger suppression on T cell proliferation and cytokine secretion than control GMSCs, while the B7-H1 blocking antibody abolished the enhanced suppression of the IFN-γ-pretreated GMSCs (Figures 4A and 4B).

We further used in vivo models to validate this finding in vitro. In line with previous studies,[4] infusion of GMSCs to CIA significantly decreased disease severity, while infusion of GMSC pretreated with IFN-γ has displayed a superior therapeutic effect on CIA, and this enhanced effect was abolished when these cells were blocked with anti-B7-H1 antibody (Figure 4C). The levels of autoantibody and the CII specific antibody showed similar changes (Figure 4D), as did cytokines (Figure S4E). The splenomegaly and lymphadenopathy in CIA mice that received GMSC pretreated with IFN-γ were less

marked than the GMSC therapeutic CIA mice (data not shown). The plasma cell, B cell, and other inflammatory cells (IFN-γ^+ CD4$^+$ T cell, IL-17a$^+$CD4$^+$ T cell) were significantly decreased in IFN-γ pretreated GMSCs compared with GMSC treatment CIA mice (Figure S4F). Micro CT imaging, hematoxylin and eosin (H&E) staining, TRAP staining, and toluidine blue staining all showed that the joint and bone damage was ameliorated to a greater extent in IFN-γ-pretreated GMSC-treated CIA mice than in GMSC-treated mice (Figure 4E). Taken together, our results indicate that IFN-γ induces the B7-H1 overexpression on GMSC and this overexpression contributes to superior therapeutic effect of GMSCs on CIA.

### B7-H1-Ameliorated GMSC Function Depends on STAT3 Signaling

We next investigated the underlying mechanism(s) by which B7-H1 on GMSCs enhances their immunosuppressive function. Phenotypically, the typical characteristic of the GMSCs did not show the differences between B7-H1^{high} and B7-H1^{low} subsets, using a flow cytometry method (Figure S5A). However, when a quantitative RT-PCR array was conducted on the B7-H1^{high} and B7-H1^{low} subsets, we found that STAT3 showed a remarkably high transcript level in B7-H1^{high} compared to B7-H1^{low} population (p < 0.0001; Figure 5A). We further explored the relevant molecules that may modulate the STAT3 signal in B7-H1^{high} GMSC. We observed that JAK/STAT3 protein expression was significantly greater in B7-H1^{high} than in B7-H1^{low} population (Figure 5B), and IFN-γ-pretreated GMSCs also increased the JAK/STAT3 expression in transcript and protein levels (Figures 5C and 5D). Conversely, the STAT3 inhibitor decreased the B7-H1 expression of the IFN-γ pretreated GMSCs (Figure 5E). We further documented that the STAT3 inhibitor significantly changed the enhanced suppression of the IFN-γ pretreated GMSC (Figure 5F) while the FasL pathway blockade did not have any effect (Figure S5B). Moreover, our chromatin immunoprecipitation (ChIP) results found that STAT3 is able to bind to the promoter region of B7-H1 and induces B7-H1 expression (Figure 5G). In CIA model mice, STAT3 pathway inhibition prevented the B7-H1 overexpressed GMSC function (Figures 5H and 5I). In general, our results suggest that JAK/STAT3 signaling is important for B7-H1 participation in GMSC-mediated immune suppression (Figure 5J).

DISCUSSION

GMSCs represent a newly identified subpopulation of MSCs that, in addition to biological features similar to other MSCs, display some unique advantages. For example, they are easily obtained and accessible from gingival tissues in the oral cavity. Additionally, these cells proliferate faster than other subsets of MSCs and sustain their homology much longer after expansion. Mostly importantly, GMSCs are not

---

scores of CIA mice changed with time. (D) The anti-dsDNA antibody, anti-CII antibody levels of the CIA mice were detected using ELISA. (E) The cytokines levels of the serum from the CIA mice were quantified by CBA kit. (F) Representative gross look, micro CT, H&E staining, TRAP, and toluidine blue stained joint tissue sections from the 3 treatment groups. CIA mice and the scores of synovial inflammations, cartilage damage, bone erosion, and the total number of TRAP-positive cells in the field were counted in each group. (G) B7-H1 expression on GMSCs and transfected GMSCs were determined using RT-PCR. (H) B7-H1 expression on GMSCs and transfected GMSCs were determined using western blotting. (I) The suppression on T cells proliferation in different groups was determined by flow cytometry. The results represent three independent experiments (mean ± SEM), *p < 0.05, **p < 0.005, ***p < 0.0005, ****p < 0.0001 by t test or ANOVA test.
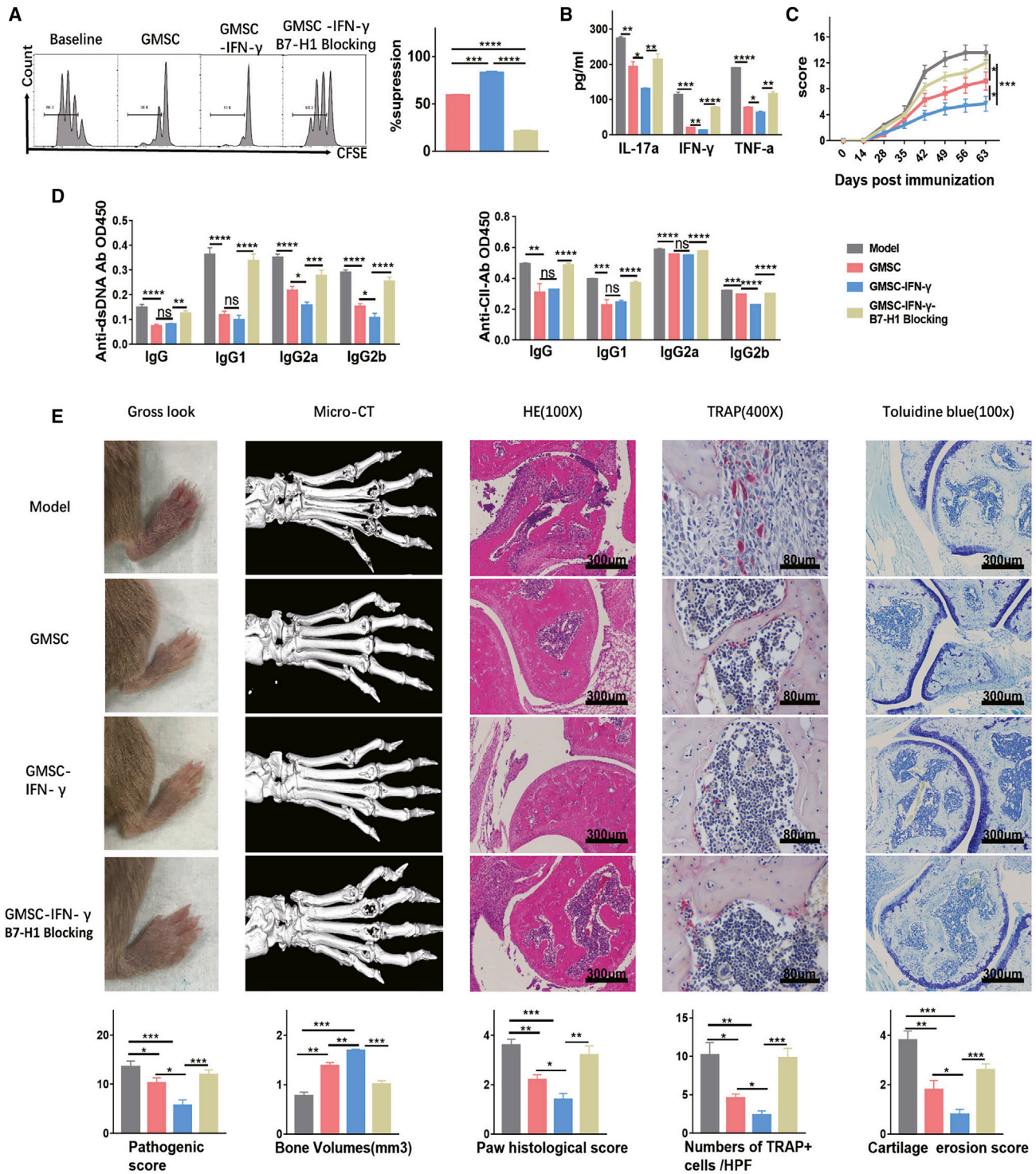
Figure 4. Overexpression of B7-H1 on GMSCs Increased the Suppression Ability of GMSCs

(A and B) GMSCs were pretreated with rh-IFN-γ (Biolegend, 10 ng/mL), with or without B7-H1 blocking antibody (Biolegend, 10 μg/mL) overnight, then co-cultured with T cells-APCs on the ratio 1:10 for 72 h. (A) The suppression on T cells proliferation in different groups was determined by flow cytometry. (B) The cytokines (IL-17a, TNF-α, and IFN-γ) secretion from T cells in different groups was determined by flow cytometry. (C–E) CIA was induced in DBA/1 mice; after 14 days of immunization, mice were treated with GMSC, IFN-γ pretreated GMSC, IFN-γ, and anti-B7-H1 antibody pretreated GMSCs or PBS (model) and euthanized on day 63, and the mice in the same group received

tumorigenic.[17] Our recent pre-clinical safety studies in mice and monkey further documented safety of these cells for clinical application for future use in the human.[42]

Due to the low immunogenicity of MSCs, it has been demonstrated that GMSCs can be successfully grafted in mouse and humanized animal models.[4,19,21] Here, we chose PDFs as control cells, because they share the similar appearance and many phenotypic features with GMSCs but they own lower immunoregulatory and regeneration abilities.[4,19] This control also shows that the results were due to GMSCs rather than to a nonspecific effect of cell rejection.

Previous studies indicate that GMSC-based immunotherapy shows therapeutic promise for treatment of RA and several other immune-mediated diseases through their properties, which decrease inflammatory T cells, dendritic cells, and macrophages and increase regulatory T cells.[18,20–23] However, the limitations of their clinical feasibility derive from the heterogeneity of GMSC, since it is unknown whether different MSC subsets possess the same range of immunomodulatory function. Some reports suggest that Toll-like receptors (TLRs) on MSCs might enhance or inhibit their immunosuppressive effects.[43,44] Additionally, another study showed that a subset of a single colony-derived MSC producing IL-17 possessed properties that could abolish MSC-based immunomodulation.[45] Therefore, more research will be required to better identify properties of different functional subsets of MSCs.

B7-H1 is a third member of the B7 family that can be induced on T cells, B cells, natural killer cells, dendritic cells, macrophages, monocytes, and some nonimmune cells including mesenchymal cells under inflammatory conditions.[34,46–49] B7-H1 also has been shown to have considerable importance for the immunosuppressive properties of BMSCs and WJMSCs.[50]

Here, we identified that B7-H1 transcriptional and translational properties were expressed to a higher degree on GMSCs compared with control cells, and especially higher on a specific GMSC cluster. Moreover, after separating GMSCs into B7-H1^{high} and B7-H1^{low} expressed subsets, we discovered that B7-H1^{high} expressed GMSCs displayed significantly more immunosuppressive activity than B7-H1^{low} expressed GMSC both *in vitro* and *in vivo* in the CIA murine model. More interestingly, blocking B7-H1 signaling on GMSCs impaired the immunomodulatory effect while overexpressing B7-H1 on GMSCs, in contrast, facilitated the immunosuppressive effect. It has to be stated here that as B7-H1 is expressed on multiple cells, we are unable to determine its specific role in GMSCs through injecting B7-H1 inhibitor to disease models. Therefore, B7-H1 may provide an excellent biomarker to identify subpopulations of GMSCs that have optimal immunoregulatory properties.

STAT3 is a transcription factor that is activated downstream of many key cytokine receptors expressed by lymphocytes, and it participates in B and T cell regulation.[51] It has been previously reported that B cell lymphoma cells release IL-10, which activates the STAT3 pathway to induce B7-H1 expression.[52] Furthermore, some reports show that STAT3 activation correlates significantly with B7-H1 expression in extranodal natural killer (NK)/T cell lymphoma cell populations.[53] In the present study, STAT3 signaling is shown to exert a significant role in strengthening the activity of B7-H1 on GMSC-mediated immunosuppression, and we document that IFN-γ promotes GMSC function due to increased B7-H1 expression via the JAK/STAT3 pathway.

In conclusion, we have demonstrated that B7-H1 plays an important role in the immunosuppressive functions of GMSC in a collagen-induced arthritis murine model that is dependent on STAT3 signaling. B7-H1 was shown to perform a crucial role in enhancing GMSC, inhibiting inflammatory immune cell activity and promoting Foxp3$^+$ Treg cell induction, thus suppressing inflammatory manifestations of the CIA model. These findings further support the notion that selecting more effective GMSC subsets, such as those exhibiting high B7-H1^{high} expression, from GMSC of similar phenotypes but with greater immunosuppressive properties, may provide a unique and additional strategy for stem cell-based therapies of autoimmune and other inflammatory diseases.

MATERIALS AND METHODS
Mice
DBA/1J (female, 8–10 weeks) were obtained from Beijing Vital River Laboratory Animal Technology and Jackson Lab. All mice were housed in the centers of experimental animals at the Sun Yat-sen University College of Medicine and the Ohio State University Wexner Medical Center. The use of animals was approved by the Institutional Animal Care and Use Committee at the Sun Yat-sen University and the Ohio State University.
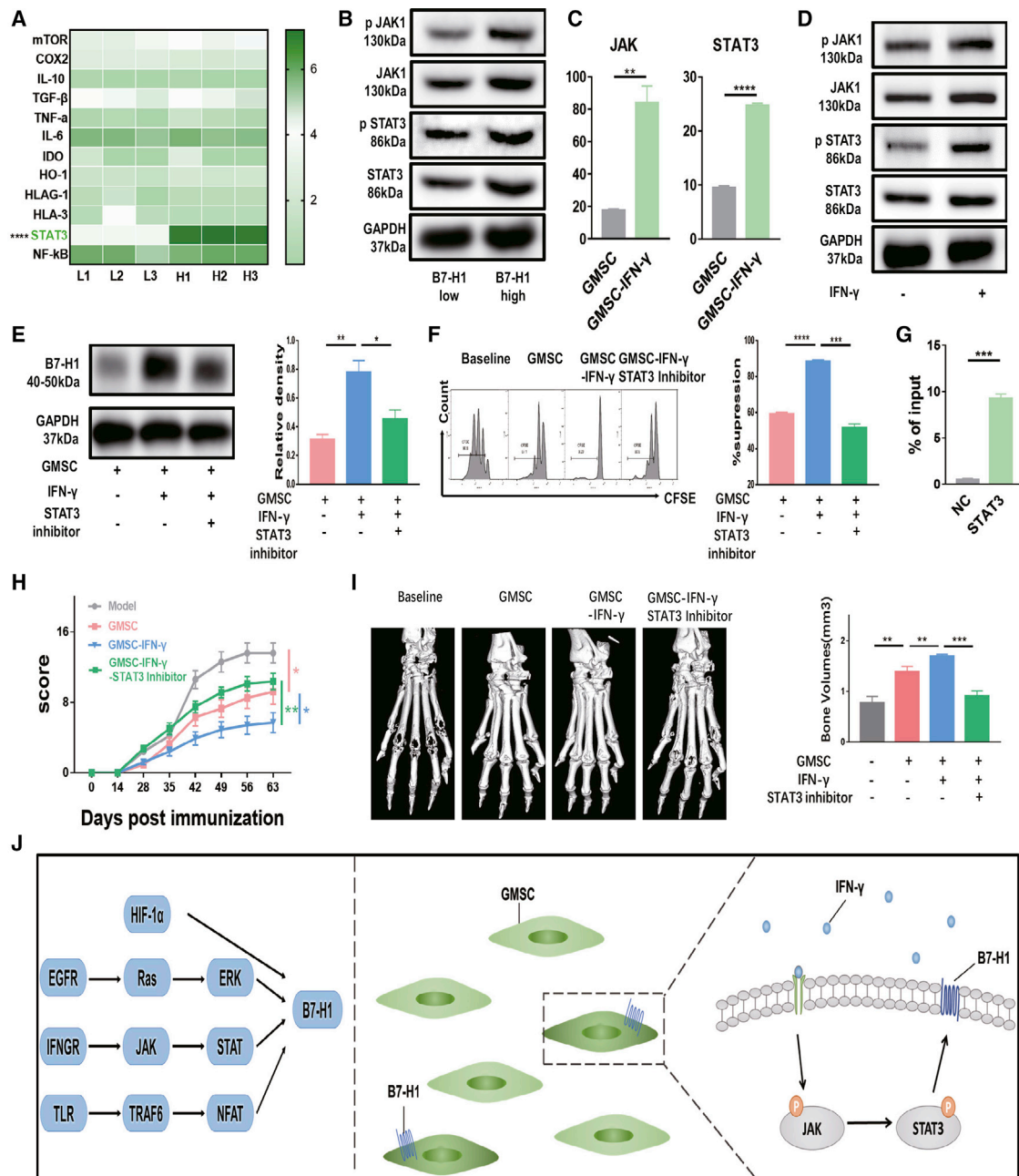
GMSCs
Human gingiva tissue samples were collected from patients undergoing routine dental procedures at the Oral and Maxillofacial Surgical Clinic in the Division of Dentistry of the Third Affiliated Hospital of Sun Yat-sen University, Guangzhou, China and Ohio State University, Columbus, OH. The PDFs were also used as a control of GMSCs. PDFs were isolated from the foreskin dermis of patients who underwent surgery. The study was approved by the Institutional Review Board (IRB) of both institutions, which permitted the collection of these specimens and the preparation of human GMSC and PDF from these samples as previously described.[4,19]

---

the same cells from the same donor (n = 5 in one individual experiment). (C) The clinical scores of CIA mice changed with time. (D) The anti-dsDNA antibody; anti-CII antibody levels of the CIA mice were detected using ELISA. (E) Representative gross look, micro CT, H&E staining, TRAP, and toluidine blue stained joint tissue sections from the CIA groups mice and the scores of synovial inflammations, cartilage damage, bone erosion, and the total number of TRAP-positive cells in the field were counted in each group. The results represent three independent experiments (mean ± SEM), *p < 0.05, **p < 0.005, ***p < 0.0005, ****p < 0.0001 by t test or ANOVA test.

Figure 5. B7-H1 Ameliorated GMSC Function through JAK/STAT3 Pathway

(A–D) GMSCs derived from three different individuals. Fresh cells or resuscitated stored cells from the third to the fifth passages were used in the experiments. (A) Quantitative RT-PCR array of the B7-H1^high GMSCs and B7-H1^low GMSCs. (B) Western blotting of the JAK/STAT3 levels of the B7-H1^high GMSCs and B7-H1^low GMSCs. (C) Quantitative RT-PCR of the JAK/STAT3 levels of the GMSCs and IFN-γ-pretreated GMSCs. (D) Western blotting of the JAK/STAT3 levels of the GMSCs and IFN-γ-pretreated GMSCs. (E) Western blotting of the B7-H1 level of the GMSCs and IFN-γ-pretreated GMSCs with or without STAT-3 inhibitor. The relative density to GAPDH was shown. (F) GMSCs were pretreated with rh-IFN-γ (Biolegend, 10 ng/mL), with or without STAT-3 inhibitor (SELLECK, 10 μM) overnight, then co-cultured with T cells-APCs on the ratio 1:10 for 72 h. The suppression on T cells proliferation in different groups was determined by flow cytometry. (G) The ChIP-qPCR analysis of the relative enrichment of STAT3 at B7-H1 promoter region. (H and I) CIA was induced in DBA/1 mice, after 14 days of immunization, mice were treated with GMSCs, IFN-γ-pretreated GMSCs, IFN-γ, and STAT-3 inhibitor pretreated GMSCs or PBS (model) and euthanized on day 63, and the mice in the same group received the same cells from the same donor (n = 5 in one individual experiment). (H) The clinical scores of CIA mice changed with time. (I) Representative micro CT of the joint tissue from different groups CIA mice. (J) Schematic of the working hypothesis. The results represent three independent experiments (mean ± SEM), *p < 0.05, **p < 0.005, ***p < 0.0005, ****p < 0.0001 by t test or ANOVA test.

CIA Model

CIA was induced by immunization of type II collagen (C II) and complete Freund's adjuvant (CFA) in DBA/1J mice as previously described[5] and described in greater detail below. On day 14 after initial CII immunization, 2×10^6 GMSCs were intravenously injected into the CIA. B7-H1^{high} GMSCs and B7-H1^{low} GMSC subsets were sorted by flow cytometry sorter and 10^7 cells/mL were suspended in in PBS and then injected into the CIA mice. GMSC were pretreated with B7-H1 blocking antibody (Biolegend, 10 μg/mL), rh-IFN-γ (Biolegend, 10 ng/mL), or STAT-3 inhibitor (SELLECK, 10 μM) and washed twice with RPMI 1640 (Hyclone) containing 10% heat-inactivated fetal bovine serum (Hyclone), 100 IU/mL penicillin (GIBCO), 1% sodium pyruvate (Corning), and 1% HEPES (Corning) before the GMSC were used in the *in vitro* and *in vivo* experiments described below. GMSC that had been used at each time point were obtained from different donors and mice in each experimental time interval received the same cell population from the same donor. Five mice were used in each group and the animal experiments were repeated at least three times.

Adoptive Transfer Colitis Model

For T cell-induced colitis, methods were followed as outlined previously.[54,55] Naive CD4$^+$ cells from C57BL/6 mice were adoptively transferred into $Rag1^{-/-}$ mice, and weight loss was monitored. The mice were euthanized at 6 weeks after the cell transfer and analyzed for disease severity.

In Vitro Suppression Assays

To examine the suppressive activity of the GMSC *in vitro*, we isolated mouse splenic T cells and antigen-presenting cells (APCs) with nylon wool. T cells labeled with CFSE were stimulated with anti-CD3 mAb (Biolegend, 1 μg/mL) and mitomycin (Sigma, M4287) pretreated APCs. GMSC were co-cultured with T cells-APCs at a ratio of 1:10. T cell proliferation ability was tested by CSFE dilution using flow cytometry, and the supernatants were collected to quantitate cytokine secretion.

Transfection

Reverse transfection was used for knockdown according to the manufacturer's protocol (Polyplus transfection) using siRNA. GMSCs were transfected with 10 nM B7-H1 siRNA (sequences 5′-GGTGTAGCACTGACATTCA-3′) or non-targeting siRNA using INTERFER in transfection reagent for 48 h. After 48 h transfection, GMSCs were washed and cultured in normal growth medium before use.

Flow Cytometric Analysis

For flow analysis, cells were prepared in single-cell suspensions. Antibodies against human B7-H1 and isotype immunoglobulin G (IgG) were from Biolegend. Antibodies against mouse CD3, CD4, CD8, CD19, B220, CD38, CD138, IFN-γ, IL-17a, Foxp3, Helios, and isotype were from Biolegend. Results were obtained on a BD FACS Fortessa flow cytometer and analyzed using FlowJo.

Cytokine Analysis

Cell culture supernatants were collected from cell culture well plates at the indicated time points and sera were collected from the different groups of CIA mice. IFN-γ, TNF, IL-17a, IL-2, IL-4, IL-6, and IL-10 concentrations were measured using a CBA kit (BD Biosciences). T cells were isolated from spleens and draining lymph nodes of the CIA mice at day 63 after CII immunization. The cells were then stimulated with PMA (Sigma, P8139), inomycin (Sigma, I0634) and Brefeldin A (Biolegend, 10 μg/mL) for 4 h, and intracellular IFN-γ and IL-17a expression were analyzed by flow cytometry.

Induction and Evaluation of Arthritis

As previously described,[4] the CIA model was induced by immunizing CII/CFA to 8- to 10-week-old female DBA/1J mice. CII (Chondrex, 20022) was emulsified with an equal volume of complete Freund's adjuvant (Sigma, F5506) containing 4 mg/mL heat-denatured mycobacterium (Difco, 231141). DBA/1J mice were immunized via intradermal injection at the tail with 50 μL of emulsion (CII 100 μg/mouse). Disease severities were monitored every 7 days following transfer of GMSC. Each paw was evaluated and scored individually using a 0–4 scoring system, and the paw scores were summed to yield an individual mouse score, with a maximum score of 16.

Micro CT Imaging

Micro CT imaging was performed using Siemens Inveon CT Scanner and Inveon Acquisition workplace software. The dataset was loaded into Amira and viewed using the Voltex display and the VolrenRed Psewdo-color Scale. Micro CT scoring: three volumes of interest were set with ± 1 mm length in the distal and proximal direction from the center of each metatarsophalangeal joint. The bone volumes of the three metatarsophalangeal joints were then calculated.

Immunohistochemistry of Joints

Mice were sacrificed at day 63 post CII immunization and the hind limbs were removed, fixed in formalin, embedded in paraffin, sectioned, and stained with H&E and toluidine blue. TRAP staining was conducted to assess osteoclasts that play a key role in bone erosion in rheumatoid arthritis and was performed with a TRAP kit (Sigma-Aldrich, 387A). All slides were evaluated by investigators blinded to the experimental conditions. H&E scoring: grade 0, no signs of inflammation; 1, mild inflammation with hyperplasia of the synovial lining without cartilage destruction; 2 through 4, increasing degrees of inflammatory cell infiltration and bone/cartilage destruction. Toluidine blue scoring: 0, normal; 1, loss of toluidine blue staining with no chondrocyte degeneration/loss and/or matrix disruption; 5, loss of toluidine blue staining with severe (depth to subchondral bone) chondrocyte loss and matrix loss in affected joints.

ELISA

Anti-ds-DNA or specific anti-CII antibodies were detected by an ELISA. 96-well plates were coated with 200 μg/mL salmon DNA or CII overnight at 37°C. After washing four times with PBS containing 0.05% Tween-20 (Sigma), and then blocked with 10% fetal bovine serum (Hyclone) in PBS for 1 h, then diluted the serum 100-fold in

1% BSA. The samples were added and incubated for 2 h at room temperature and washed once and primed with horseradish peroxidase (HRP)-conjugated goat anti-mouse IgG, IgG1, IgG2a, or IgG2b antibody. After washing several times, the color development was primed with tetramethylbenzidine (TMB) (Sigma-Aldrich), the reaction was stopped by 0.5 M H_2SO_4, and absorbance at 450 nm was measured in a microplate reader (Bio-Rad).

Immunofluorescence Staining
The cell slides were fixed in 1% PFA for 15 min at room temperature (RT), followed by permeabilization in 0.5% Triton X-100 for 20 min. They were blocked in 6% BSA in PBS-T (PBS containing 0.3% Tween) and incubated with primary antibody (CST, #13684) overnight. The slides were then washed twice in PBS-T and incubated with secondary antibodies (Alexa Fluor 488 goat anti-rabbit IgG; 1:1,000 in 0.03% BSA) for 2 h before final washes in PBS-T, and high resolution images were obtained using a Leica confocal microscope equipped with a $100\times$ objective lens (Leica).

Western Blotting
GMSCs were collected and lysed using commercial buffer (Sigma). Protein extracts were separated by 10% polyacrylamide-SDS gels and electroblotted onto nitrocellulose membranes (Gene Script). After blocking with 5% nonfat dry milk/TBS, the membranes were incubated with antibodies against STAT3, JAK1, phosphorite STAT3, JAK1, and B7-H1 (Cell Signaling Technology), followed by incubation with HRP-conjugated secondary antibody (Cell Signaling Technology). The blots were then reported with GAPDH antibody (Cell Signaling Technology).

RT-PCR
Total RNA was extracted from GMSC with a RNeasy Mini Kit (Omega, R6834-2), and cDNA was generated by using a PrimeScript-RT-PCR Kit (TAKARA). B7-H1, mTOR, COX2, IL-10, transforming growth factor-β (TGF-β), TNF-α, IL-6, indoleamine2,3-dioxygenase (IDO), heme oxygenase 1 (HO-1), human leukocyte antigen G 1 (HLAG-1), human leukocyte antigen 3 (HLA-3), signal transducer and activator of transcription 3 (STAT-3), nuclear factor κB (NF-κB) mRNA expression was quantified by using the SYBP○R Premix Ex Taq II Kit (TAKARA). The samples were performed in triplicate, and the relative expression of the above molecules was determined by normalizing the expression of each target gene to β-actin by using the $2^{-\Delta\Delta Ct}$ method.

ChIP
ChIP was carried out using an anti-STAT3 antibody (Cell Signaling Technology) and chromatin extracts equivalent to 10^6 cells. ChIP samples were quantified by RT-PCR Kit (TAKARA) and the ChIP PCR data were normalized using the percent input method. The sequences of primers are as follows: human B7-H1 promoter forward 5′-TGGACTGACATGTTTCACTTTCT-3′, human B7-H1 promoter reverse 5′-CAAGGCAGCAAATCCAGTTT-3′.

RNA Sequence and Single Cell Sequence
Total RNA was extracted with the RNeasy mini kit (Invitrogen). The RNA degradation and contamination was monitored on 1% agarose gels, and its quality was assessed using the Nanodrop3000. cDNA library construction and Illumina sequencing were completed by Beijing Novogene Bioinformatics Technology. Briefly, sequencing libraries were generated using NEBNext Ultra RNA Library Prep Kit following the manufacturer's recommendations. PCR products were purified (AMPure XP system) and library quality was assessed on the Agilent Bioanalyzer 2100 system. The library preparations were sequenced on Illumina Hiseq 2000 platform, and 125 bp/150 bp paired-end reads were generated. Single cells were encapsulated into emulsion droplets using Chromium Controller (10× Genomics). Single cell sequence libraries were constructed using Chromium Single Cell 30 v2 Reagent Kit according to the manufacturer's protocol. RNA-seq data used in this study is available at the NCBI SRA database under accession number PRJNA540091.

Statistical Analysis
For comparison of treatment groups, we performed unpaired-t tests or paired-t tests, as indicated. All statistical analyses were performed using GraphPad Prism software. A p value <0.05 is considered as statistically significant.

SUPPLEMENTAL INFORMATION
Supplemental Information can be found online at https://doi.org/10.1016/j.ymthe.2020.07.002.

AUTHOR CONTRIBUTIONS
S.G.Z. designed the research; W.W. and Z.X.X. performed the experiments; W.W., Z.X.X., and S.G.Z. wrote the manuscript; D.Z. and F.H. provided gingival tissues; J.W. provide assistance and guidance on experiments; Y.L. provided assistance in single cell sequence; J.A.B. and N.O. contributed to writing and editing the manuscript. All the authors read and approved the final version.

CONFLICTS OF INTEREST
The authors declare no competing interests.

ACKNOWLEDGMENTS

REFERENCES
1. American College of Rheumatology Ad Hoc Committee on Clinical Guidelines (1996). Guidelines for the management of rheumatoid arthritis. Arthritis Rheum. 39, 713–722.

2. Firestein, G.S. (2003). Evolving concepts of rheumatoid arthritis. Nature 423, 356–361.

3. Smolen, J.S., Aletaha, D., and McInnes, I.B. (2016). Rheumatoid arthritis. Lancet 388, 2023–2038.

4. Chen, M., Su, W., Lin, X., Guo, Z., Wang, J., Zhang, Q., Brand, D., Ryffel, B., Huang, J., Liu, Z., et al. (2013). Adoptive transfer of human gingiva-derived mesenchymal stem cells ameliorates collagen-induced arthritis via suppression of Th1 and Th17 cells and enhancement of regulatory T cell differentiation. Arthritis Rheum. 65, 1181–1193.

5. Kong, N., Lan, Q., Su, W., Chen, M., Wang, J., Yang, Z., Park, R., Dagliyan, G., Conti, P.S., Brand, D., et al. (2012). Induced T regulatory cells suppress osteoclastogenesis and bone erosion in collagen-induced arthritis better than natural T regulatory cells. Ann. Rheum. Dis. 71, 1567–1572.

6. Pittenger, M.F., Mackay, A.M., Beck, S.C., Jaiswal, R.K., Douglas, R., Mosca, J.D., Moorman, M.A., Simonetti, D.W., Craig, S., and Marshak, D.R. (1999). Multilineage potential of adult human mesenchymal stem cells. Science 284, 143–147.

7. Xu, J., Zhang, D., Zanvit, P., and Wang, D. (2018). The Immunomodulatory Properties of Mesenchymal Stem Cells. Stem Cells Int. 2018, 9214831.

8. Nauta, A.J., and Fibbe, W.E. (2007). Immunomodulatory properties of mesenchymal stromal cells. Blood 110, 3499–3506.

9. Uccelli, A., Moretta, L., and Pistoia, V. (2008). Mesenchymal stem cells in health and disease. Nat. Rev. Immunol. 8, 726–736.

10. Jarvinen, L., Badri, L., Wettlaufer, S., Ohtsuka, T., Standiford, T.J., Toews, G.B., Pinsky, D.J., Peters-Golden, M., and Lama, V.N. (2008). Lung resident mesenchymal stem cells isolated from human lung allografts inhibit T cell proliferation via a soluble mediator. J. Immunol. 181, 4389–4396.

11. Kim, J., and Hematti, P. (2009). Mesenchymal stem cell-educated macrophages: a novel type of alternatively activated macrophages. Exp. Hematol. 37, 1445–1453.

12. Spaggiari, G.M., Abdelrazik, H., Becchetti, F., and Moretta, L. (2009). MSCs inhibit monocyte-derived DC maturation and function by selectively interfering with the generation of immature DCs: central role of MSC-derived prostaglandin E2. Blood 113, 6576–6583.

13. Spaggiari, G.M., Capobianco, A., Abdelrazik, H., Becchetti, F., Mingari, M.C., and Moretta, L. (2008). Mesenchymal stem cells inhibit natural killer-cell proliferation, cytotoxicity, and cytokine production: role of indoleamine 2,3-dioxygenase and prostaglandin E2. Blood 111, 1327–1333.

14. Zhang, Q.Z., Su, W.R., Shi, S.H., Wilder-Smith, P., Xiang, A.P., Wong, A., Nguyen, A.L., Kwon, C.W., and Le, A.D. (2010). Human gingiva-derived mesenchymal stem cells elicit polarization of m2 macrophages and enhance cutaneous wound healing. Stem Cells 28, 1856–1868.

15. Fan, X.L., Zeng, Q.X., Li, X., Li, C.L., Xu, Z.B., Deng, X.Q., Shi, J., Chen, D., Zheng, S.G., and Fu, Q.L. (2018). Induced pluripotent stem cell-derived mesenchymal stem cells activate quiescent T cells and elevate regulatory T cell response via NF-κB in allergic rhinitis patients. Stem Cell Res. Ther. 9, 170.

16. Zhang, Q., Shi, S., Liu, Y., Uyanne, J., Shi, Y., Shi, S., and Le, A.D. (2009). Mesenchymal stem cells derived from human gingiva are capable of immunomodulatory functions and ameliorate inflammation-related tissue destruction in experimental colitis. J. Immunol. 183, 7787–7798.

17. Tomar, G.B., Srivastava, R.K., Gupta, N., Barhanpurkar, A.P., Pote, S.T., Jhaveri, H.M., Mishra, G.C., and Wani, M.R. (2010). Human gingiva-derived mesenchymal stem cells are superior to bone marrow-derived mesenchymal stem cells for cell therapy in regenerative medicine. Biochem. Biophys. Res. Commun. 393, 377–383.

18. Huang, F., Liu, Z.M., and Zheng, S.G. (2018). Updates on GMSCs Treatment for Autoimmune Diseases. Curr. Stem Cell Res. Ther. 13, 345–349.

19. Luo, Y., Wu, W., Gu, J., Zhang, X., Dang, J., Wang, J., Zheng, Y., Huang, F., Yuan, J., Xue, Y., et al. (2019). Human gingival tissue-derived MSC suppress osteoclastogenesis and bone erosion via CD39-adenosine signal pathway in autoimmune arthritis. EBioMedicine 43, 620–631.

20. Su, W.R., Zhang, Q.Z., Shi, S.H., Nguyen, A.L., and Le, A.D. (2011). Human gingiva-derived mesenchymal stromal cells attenuate contact hypersensitivity via prostaglandin E2-dependent mechanisms. Stem Cells 29, 1849–1860.

21. Huang, F., Chen, M., Chen, W., Gu, J., Yuan, J., Xue, Y., Dang, J., Su, W., Wang, J., Zadeh, H.H., et al. (2017). Human Gingiva-Derived Mesenchymal Stem Cells Inhibit Xeno-Graft-versus-Host Disease via CD39-CD73-Adenosine and IDO Signals. Front. Immunol. 8, 68.

22. Zhang, W., Zhou, L., Dang, J., Zhang, X., Wang, J., Chen, Y., Liang, J., Li, D., Ma, J., Yuan, J., et al. (2017). Human Gingiva-Derived Mesenchymal Stem Cells Ameliorate

23. Zhang, X., Huang, F., Li, W., Dang, J.L., Yuan, J., Wang, J., Zeng, D.L., Sun, C.X., Liu, Y.Y., Ao, Q., et al. (2018). Human Gingiva-Derived Mesenchymal Stem Cells Modulate Monocytes/Macrophages and Alleviate Atherosclerosis. Front. Immunol. 9, 878.

24. Zhao, J., Chen, J., Huang, F., Wang, J., Su, W., Zhou, J., Qi, Q., Cao, F., Sun, B., Liu, Z., et al. (2019). Human gingiva tissue-derived MSC ameliorates immune-mediated bone marrow failure of aplastic anemia via suppression of Th1 and Th17 cells and enhancement of CD4+Foxp3+ regulatory T cells differentiation. Am. J. Transl. Res. 11, 7627–7643.

25. Wu, Wenbin, et al. (2020). CD39 Produced from Human GMSCs Regulates the Balance of Osteoclasts and Osteoblasts through the Wnt/β-Catenin Pathway in Osteoporosis. Mol. Ther.

26. Tyndall, A. (2011). Successes and failures of stem cell transplantation in autoimmune diseases. Hematology (Am. Soc. Hematol. Educ. Program) 2011, 280–284.

27. Phinney, D.G. (2012). Functional heterogeneity of mesenchymal stem cells: implications for cell therapy. J. Cell. Biochem. 113, 2806–2812.

28. Kalinina, N., Kharlampieva, D., Loguinova, M., Butenko, I., Pobeguts, O., Efimenko, A., Ageeva, L., Sharonov, G., Ischenko, D., Alekseev, D., et al. (2015). Characterization of secretomes provides evidence for adipose-derived mesenchymal stromal cells subtypes. Stem Cell Res. Ther. 6, 221.

29. Rennerfeldt, D.A., and Van Vliet, K.J. (2016). Concise Review: When Colonies Are Not Clones: Evidence and Implications of Intracolony Heterogeneity in Mesenchymal Stem Cells. Stem Cells 34, 1135–1141.

30. Taube, J.M., Anders, R.A., Young, G.D., Xu, H., Sharma, R., McMiller, T.L., Chen, S., Klein, A.P., Pardoll, D.M., Topalian, S.L., and Chen, L. (2012). Colocalization of inflammatory response with B7-h1 expression in human melanocytic lesions supports an adaptive resistance mechanism of immune escape. Sci. Transl. Med. 4, 127ra37.

31. Sanmamed, M.F., and Chen, L. (2014). Inducible expression of B7-H1 (PD-L1) and its selective role in tumor site immune modulation. Cancer J. 20, 256–261.

32. Dong, H., Zhu, G., Tamada, K., and Chen, L. (1999). B7-H1, a third member of the B7 family, co-stimulates T-cell proliferation and interleukin-10 secretion. Nat. Med. 5, 1365–1369.

33. Tsushima, F., Yao, S., Shin, T., Flies, A., Flies, S., Xu, H., Tamada, K., Pardoll, D.M., and Chen, L. (2007). Interaction between B7-H1 and PD-1 determines initiation and reversal of T-cell anergy. Blood 110, 180–185.

34. Yao, S., and Chen, L. (2014). PD-1 as an immune modulatory receptor. Cancer J. 20, 262–264.

35. Luz-Crawford, P., Noël, D., Fernandez, X., Khoury, M., Figueroa, F., Carrión, F., Jorgensen, C., and Djouad, F. (2012). Mesenchymal stem cells repress Th17 molecular program through the PD-1 pathway. PLoS ONE 7, e45272.

36. Wang, H., Qi, F., Dai, X., Tian, W., Liu, T., Han, H., Zhang, B., Li, H., Zhang, Z., and Du, C. (2014). Requirement of B7-H1 in mesenchymal stem cells for immune tolerance to cardiac allografts in combination therapy with rapamycin. Transpl. Immunol. 31, 65–74.

37. Yan, Z., Zhuansun, Y., Liu, G., Chen, R., Li, J., and Ran, P. (2014). Mesenchymal stem cells suppress T cells by inducing apoptosis and through PD-1/B7-H1 interactions. Immunol. Lett. 162 (1 Pt A), 248–255.

38. Ishibashi, N., Watanabe, T., Kanehira, M., Watanabe, Y., Hoshikawa, Y., Notsuda, H., Noda, M., Sakurada, A., Ohkouchi, S., Kondo, T., and Okada, Y. (2018). Bone marrow mesenchymal stromal cells protect allograft lung transplants from acute rejection via the PD-L1/IL-17A axis. Surg. Today 48, 726–734.

39. Lu, L., Lan, Q., Li, Z., Zhou, X., Gu, J., Li, Q., Wang, J., Chen, M., Liu, Y., Shen, Y., et al. (2014). Critical role of all-trans retinoic acid in stabilizing human natural regulatory T cells under inflammatory conditions. Proc. Natl. Acad. Sci. USA 111, E3432–E3440.

40. Zheng, S.G., Meng, L., Wang, J.H., Watanabe, M., Barr, M.L., Cramer, D.V., Gray, J.D., and Horwitz, D.A. (2006). Transfer of regulatory T cells generated ex vivo modifies graft rejection through induction of tolerogenic CD4+CD25+ cells in the recipient. Int. Immunol. 18, 279–289.

41. Li, N., Wang, J., Zhang, N., Zhuang, M., Zong, Z., Zou, J., Li, G., Wang, X., Zhou, H., Zhang, L., and Shi, Y. (2018). Cross-talk between TNF-α and IFN-γ signaling in

Streptozoticin-induced T1DM in mice via Suppression of T effector cells and Upregulating Treg Subsets. Sci. Rep. 7, 15249.

induction of B7-H1 expression in hepatocellular carcinoma cells. Cancer Immunol. Immunother. 67, 271–283.

42. Zhao, J., Wang, J., Dang, J., Zhu, W., Chen, Y., Zhang, X., Xie, J., Hu, B., Huang, F., Sun, B., et al. (2019). A preclinical study-systemic evaluation of safety on mesenchymal stem cells derived from human gingiva tissue. Stem Cell Res. Ther. 10, 165.

43. Liotta, F., Angeli, R., Cosmi, L., Filì, L., Manuelli, C., Frosali, F., Mazzinghi, B., Maggi, L., Pasini, A., Lisi, V., et al. (2008). Toll-like receptors 3 and 4 are expressed by human bone marrow-derived mesenchymal stem cells and can inhibit their T-cell modulatory activity by impairing Notch signaling. Stem Cells 26, 279–289.

44. Opitz, C.A., Litzenburger, U.M., Lutz, C., Lanz, T.V., Tritschler, I., Köppel, A., Tolosa, E., Hoberg, M., Anderl, J., Aicher, W.K., et al. (2009). Toll-like receptor engagement enhances the immunosuppressive properties of human bone marrow-derived mesenchymal stem cells by inducing indoleamine-2,3-dioxygenase-1 via interferon-beta and protein kinase R. Stem Cells 27, 909–919.

45. Yang, R., Liu, Y., Kelk, P., Qu, C., Akiyama, K., Chen, C., Atsuta, I., Chen, W., Zhou, Y., and Shi, S. (2013). A subset of IL-17(+) mesenchymal stem cells possesses anti-Candida albicans effect. Cell Res. 23, 107–121.

46. Mazanet, M.M., and Hughes, C.C.W. (2002). B7-H1 is expressed by human endothelial cells and suppresses T cell cytokine synthesis. J. Immunol. 169, 3581–3588.

47. Blazar, B.R., Carreno, B.M., Panoskaltsis-Mortari, A., Carter, L., Iwai, Y., Yagita, H., Nishimura, H., and Taylor, P.A. (2003). Blockade of programmed death-1 engagement accelerates graft-versus-host disease lethality by an IFN-gamma-dependent mechanism. J. Immunol. 171, 1272–1277.

48. Wiendl, H., Mitsdoerffer, M., Schneider, D., Chen, L., Lochmüller, H., Melms, A., and Weller, M. (2003). Human muscle cells express a B7-related molecule, B7-H1, with strong negative immune regulatory potential: a novel mechanism of counterbalancing the immune attack in idiopathic inflammatory myopathies. FASEB J. 17, 1892–1894.

49. Liang, S.C., Latchman, Y.E., Buhlmann, J.E., Tomczak, M.F., Horwitz, B.H., Freeman, G.J., and Sharpe, A.H. (2003). Regulation of PD-1, PD-L1, and PD-L2 expression during normal and autoimmune responses. Eur. J. Immunol. 33, 2706–2716.

50. Jang, I.K., Jung, H.J., Noh, O.K., Lee, D.H., Lee, K.C., and Park, J.E. (2018). B7-H1-mediated immunosuppressive properties in human mesenchymal stem cells are mediated by STAT-1 and not PI3K/Akt signaling. Mol. Med. Rep. 18, 1842–1848.

51. Deenick, E.K., Pelham, S.J., Kane, A., and Ma, C.S. (2018). Signal Transducer and Activator of Transcription 3 Control of Human T and B Cell Responses. Front. Immunol. 9, 168.

52. Li, L., Zhang, J., Chen, J., Xu-Monette, Z.Y., Miao, Y., Xiao, M., Young, K.H., Wang, S., Medeiros, L.J., Wang, M., et al. (2018). B-cell receptor-mediated NFATc1 activation induces IL-10/STAT3/PD-L1 signaling in diffuse large B-cell lymphoma. Blood 132, 1805–1817.

53. Song, T.L., Nairismägi, M.L., Laurensia, Y., Lim, J.Q., Tan, J., Li, Z.M., Pang, W.L., Kizhakeyil, A., Wijaya, G.C., Huang, D.C., et al. (2018). Oncogenic activation of the STAT3 pathway drives PD-L1 expression in natural killer/T-cell lymphoma. Blood 132, 1146–1158.

54. Chen, W., Xu, Z., Zheng, Y., Wang, J., Qian, W., Olsen, N., Brand, D., Lin, J., and Zheng, S.G. (2017). A protocol to develop T helper and Treg cells in vivo. Cell. Mol. Immunol. 14, 1013–1016.

55. Luo, Y., Xue, Y., Wang, J., Dang, J., Fang, Q., Huang, G., Olsen, N., and Zheng, S.G. (2019). Negligible Effect of Sodium Chloride on the Development and Function of TGF-beta-Induced CD4(+) Foxp3(+) Regulatory T Cells. Cell Rep 26, 1869–1879.